RSC Advances

ROYAL SOCIETY OF CHEMISTRY

www.rsc.org/advances

REVISED MANUSCRIPT RA-ART-01-2014-000790

Self structure formation in polyadenylic acid by small molecules: New insights from the binding of planar dyes thionine and toluidine blue O

Puja Paul and Gopinatha Suresh Kumar*

Biophysical Chemistry Laboratory, Chemistry Division

CSIR-Indian Institute of Chemical Biology

Kolkata 700 032, India

Address for Correspondence:

Dr. G. Suresh Kumar, Ph.D

Scientist

Biophysical Chemistry Laboratory

Indian Institute of Chemical Biology (CSIR)

4, Raja S. C. Mullick Road

Kolkata 700 032, INDIA

Phone: +91 33 2472 4049/2499 5723

Fax: +91 33 2473 0284 / 5197

e-mail: gskumar@iicb.res.in/gsk.iicb@gmail.com

*author to whom all correspondence should be addressed.

REVISED MANUSCRIPT RA-ART-01-2014-000790

Abstract

Self-structure induction in single stranded poly(A) is a promising approach that can switch off protein production and pave a new route for the development of RNA based therapeutic agents. Utilising spectroscopic techniques and isothermal titration calorimetric methods, we examined the ability of two DNA binding phenothiazinium dyes thionine (TH) and toluidine blue O (TB) to induce structural changes in ss poly(A). The cooperative binding of both the dyes to ss poly(A) was revealed from absorbance and fluorescence studies. The binding affinity were of the order of 10^6 M^{-1} at 50 mM [Na^+] as determined from spectroscopic and calorimetric studies. Ferrocyanide quenching studies showed intercalative binding of the dyes to poly(A). The binding perturbed the circular dichroism spectrum of poly(A) with concomitant formation of prominent induced CD bands in the 300-700 nm region for the dyes. Poly(A) forms self-structure with a in the presence of bothe TH and TB. The binding affinity and the ease of formation of self structure enhanced with [Na^+] ion concentration in the presence of dyes in the range 50-200 mM. The single stranded poly(A) binding affinity of TH is higher compared to TB. Poly(A) may be a potential bio-target of these dyes in their pharmacological application.

Keywords: Phenothiazinium dyes, Spectroscopy, Self structure, Intercalation

REVISED MANUSCRIPT RA-ART-01-2014-000790

Introduction

The knowledge of the essential roles of RNA in normal biological processes and in the progression in many diseases has led to growing interest in exploiting RNA as a target for therapeutic intervention. Consequently, in the last few years, there has been a paradigm shift to develop small molecules that can be targeted to various RNA structures in order to develop RNA targeted antibiotics for therapeutic use. New drugs developed must be able to specifically bind to unique structural organizations in RNA to regulate the gene expression.

Polyadenylic acid has been the focus of increasing attention for its role in mRNA functioning. All eukaryotic mRNAs have a long poly(A) tail at the 3' end that is added during post transcriptional modification of the mRNA.[1-3] The long poly(A) tail is an important determinant of mRNA stability and maturation, and is essential for the initiation of translation. Poly(A) polymerase (PAP) that catalyzes 3'-end poly(A) synthesis, participates in an endonucleolytic cleavage step, and is one key factor in the polyadenylation of the 3'-end of mRNA. Neo-PAP, a recently identified human PAP, is significantly over expressed in human cancer cells in comparison to its expression in normal cells.[4] It has also been suggested that the poly(A) tails of mRNA may represent a malignancy specific target.[2] Drugs capable of recognizing and binding to the single-stranded (ss) poly(A) tail of mRNA may interfere with the full processing of mRNA by PAP and would represent a new type of RNA targeed therapeutic agent.

Polyriboadenylic acid has the unique characteristics of existing as a single stranded helical structure and parallel stranded double stranded helix,[5-6] the later being stabilized at acid pH by base paired protonated adenines. Recently, many small molecules have been reported to induce a unique self-structure in poly(A) at neutral pH where only the ss structure can otherwise exist.[7-17] The mechanism of such self-structure formation at physiological pH, the nature and mode of the

REVISED MANUSCRIPT RA-ART-01-2014-000790

transition, the features of the small molecules that can specifically induce this novel conformational transition and the structure of the self-structure by itself are still obscure.[7-17] Apparently, more elaborate studies with various compounds are required to understand this peculiar phenomenon of nucleic acid self -structural reorganization.

Thionine (TH) and toluidine blue O (TB) are the two most common phenothiazinium dyes; they differ in the groups present at 2, 3 and 7 positions (Fig. 1a,b). Thionine (3,7-Diamino-5-phenothiazinium), a tricyclic heteroaromatic molecule, has been studied for its intercalative interaction, toxic effects,[18] photoinduced mutagenic actions on binding to DNA[19] and photoinduced inactivation of viruses.[20] TH has been shown to inactivate frog sperm nucleus,[21] produce toxic effects in anaerobic glycolysis,[22] induce structural changes in rat mast cells and block mast cell damage by inhibiting cell metabolism.[23] Nitrite ion,[24] rhodium,[25] nickel[26] which are hazardous environmental pollutants are determined spectrophotometrically by use of cationic dye like thionine.

TB (2-methyl-3-dimethylamino-7-amino-phenothiazin-5-iumchloride), a blue cationic (basic) dye has been explored by Ames test to have mutagenic effect.[27] Many reports suggest that TB, like TH has several toxic effects. Popa and Bosch[28] reported the toxic interaction of TB and RNA by gel electrophoresis and spectrophotometry. The use of visible light in conjunction with an appropriate photosensitizers like MB/TB may be a useful alternative and/or adjuvant to antibiotics and antiseptics for skin conditions associated with microbial etiology.[29] According to the report of Ephros and Mashberg, the use of TB as a mouth rinse and subsequent flushing to the environment presents potentially serious consequences that might adversely affect fish and other aquatic life.[30] Because TB reacts with ribonucleic acids, Wysocki[31] ascribed a possible

REVISED MANUSCRIPT RA-ART-01-2014-000790

mutagenic effect to TB, especially when vitally stained cells are exposed to high-energy irradiation.

Using spectrophotometric, spectroflorimetric, spectropolarimetric and thermal melting studies the potential of these two important phenothiazinium dyes to interact with ss poly(A) and induce self-structure has been probed in a search of promising lead compounds for controlling the poly(A) chain elongation and mRNA degradation. The spectroscopic results are supplemented with thermodynamic data from high sensitivity isothermal titration calorimetry. This research on the interaction of TH and TB to poly(A) at molecular level is not only helpful for elucidating the basic information of pharmacological actions, but also can further elaborate the toxic effects of the dyes on poly(A) function.

Results and discussion

Spectrophotometric studies

Changes in the visible absorption spectra of the dyes occurred as a result of titration with increasing concentration of ss poly(A) in the 450-700 nm region. The maximum absorbance of TH and TB located around 598 nm (with a shoulder at 557 nm) and 618 nm, respectively, were chosen to monitor the interaction as ss poly(A) does not absorb in this wavelength. The spectrum '1' of Fig. 2 a,b are the absorption spectra of free TO and TB molecule, respectively, that underwent hypochromic effect on titration with increasing P/D (nucleotide phosphate/dye molar ratio). Hypochromism is assigned to a strong interaction between the electronic states of the interacting chromophore and that of the poly(A) bases. A bathochromic shift of ~4 nm concomitant with the appearance of a sharp isosbestic point at 613 nm occurred in case of TH. The red shift which was observed upon TH binding to poly(A), is consistent with the $\pi - \pi^*$ stacking of the dye with the adenine bases, such as that occurs upon intercalation. Similar type of

REVISED MANUSCRIPT RA-ART-01-2014-000790

spectral changes were observed when interaction of TH was studied with DNA and tRNA.[32-33] But TB-ss poly(A) interaction yielded two isosbestic points at 531 and 571 nms, respectively, in contrast to that with TB-DNA and TB-tRNA interaction.[32-33] These spectral changes in the dyes may also reflect changes of ss poly(A) conformation and structures after the dye binding. The isosbestic point enabled the assumption of a two state system consisting of bound and free dye at any particular wavelength enabling equilibrium conditions in the dye-ss poly(A) complexation. Titration of a constant concentration of ss poly(A) with increasing concentration of the dyes was also performed in each case for evaluating the free and bound dyes at several inputs of the ss poly(A). The spectral changes were utilized to construct a Scatchard plot of r/C_f versus r to quantify the binding reaction. The optical properties of the free and poly(A) bound dye molecules are presented in Table S1.

Fluorescence titration studies

TH and TB have strong intrinsic fluorescence with emission spectra in the 600-700 nm range with maxima centered at 615 nm and 638 nm, respectively, when excited at 596 nm and 620 nm. Complex formation was monitored by titration studies keeping constant concentration of the dyes and increasing the concentration of poly(A). With increasing concentration of poly(A), progressive quenching of the fluorescence of TH and TB was observed eventually reaching a saturation point without any shift in the wavelength maxima (Fig. 2 c,d).

Evaluation of the binding affinity

The results of the spectrophotometric (Fig. 3 a,b) and spectrofluorimetric (Fig. 3 c,d) titrations were analyzed by constructing Scatchard plots. The Scatchard plots exhibited cooperative behavior as revealed by positive slope at low r values and hence were analyzed further by the McGhee-von Hippel methodology[34] for cooperative binding using equation (1) for evaluation of

REVISED MANUSCRIPT RA-ART-01-2014-000790

the binding constants. The cooperative binding affinity (K) values of TH and TB to poly(A) were evaluated to be (2.66±0.02) × 10^5 M^{-1} and (0.67±0.03) × 10^5 M^{-1}, respectively, from absorbance data and (2.28±0.04) × 10^5 M^{-1} and (0.64±0.01) × 10^5 M^{-1}, respectively, from fluorescence data. These values and the number of binding sites, and the cooperativity factors (ω) are depicted in Table 1. The apparent binding constant ($K_i\omega$) which is a product of the cooperative binding affinity and the cooperative factor gave values of (5.32±0.02) ×10^6 M^{-1} and (5.24±0.04) × 10^6 M^{-1}, respectively, for TH and (4.02±0.03) ×10^6 M^{-1} and (3.97±0.01) × 10^6 M^{-1}, respectively, for TB from spectrophotometry and spectrofluorimetry data indicating high binding affinity for TH in comparison to TB to poly(A). The differences in the functional domains of the two molecules may be responsible for the small differences in the binding affinity.

Binding stoichiometry determination (Job plot)

The stoichiometry of the association of the dyes to ss poly(A) was determined by the continuous variation analysis of Job from fluorescence data. The plot of the difference in fluorescence intensity (ΔF) at 615 nm and 638 nm, respectively, for TH and TB versus the mole fraction of the corresponding dyes revealed a single binding mode in each case (Fig. S1, ESI).

From the inflection points, χ_{TO}= 0.299 and χ_{TBO}= 0.281, the number of nucleotides bound per TH and TB were estimated to be around 2.34 and 2.55, respectively. These values are closely similar to the number of binding sites evaluated from the spectroscopic data. The model of binding that can be envisaged here is classical intercalation. As a consequence of the intercalation, the "neighbour exclusion principle" persists in the dye-poly(A) complex. Simple classical intercalators show saturation with nucleic acid at a stoichiometry of one dye molecule per 2 base pairs. Hence, there is a maximum of one intercalator between every three potential binding site leading to exclusion of two potential sites one each on top and bottom of the bound site. Apart

REVISED MANUSCRIPT RA-ART-01-2014-000790

from the pushing of the base pairs on the above and below leading to reduction of space, the intercalator binding induces conformational changes at adjacent sites of nucleic acid and the new conformation is structurally or sterically unable to access another intercalator to the binding site next to the neighboring intercalation pockets. Electrostatic repulsion between proximally bound dyes may also contribute to this phenomenon. The phenomenon becomes more relevant as the binding leads to self structure formation (*vide infra*).

Fluorescence quenching studies

Fluorescence quenching experiments provide an effective method for investigating the binding of small molecules to nucleic acid structure. The intercalation phenomena involve the entrapment of the dye between bases of nucleic acid, in such a way that the helical structure is able to protect the bound molecules from a possible quencher. In the complex, molecules that are free or bound on the surface of the poly(A) may be readily available to an anionic quencher like $[Fe(CN)_6]^{4-}$, while those bound inside may be shielded. The electrostatic barrier due to the negative charges on the phosphate groups at the helix surface limits the penetration of an anionic quencher into the helix. Therefore, a small molecule bound in an intercalative mode should be protected from being quenched by the anionic quencher, and the magnitude of K_{sv} of the bound molecules should vary considerably than that of the free small molecules. In contrast, externally bound and groove bound molecules may be quenched readily by anionic quenchers, and the magnitude of K_{sv} of such molecules should be nearly same to that of the free ones. Stern-Volmer plots for the quenching of TH and TB fluorescence complexed with ss poly(A) are shown in Fig. S2, ESI. In the presence of $[Fe(CN)_6]^{4-}$, K_{sv} values for free TH and its complex with ss poly(A) were 41 and 5.7 M^{-1}, respectively, and the same for TB were 36 and 5.4 M^{-1}. The percentage of quenching was more (~72%) in the case of TH-ss poly(A) complex compared to that for TB-ss

REVISED MANUSCRIPT RA-ART-01-2014-000790

poly(A) complex (~67%) with respect to the free dyes. This indicates that the binding of TH to poly(A) is hindered to some extent the accessibility of the quencher to the bound ligand molecules suggesting a better stacking interaction of TH inside the polynucleotide, or in other words bound ligand molecules are considerably protected and sequestered away from the solvent suggesting stronger binding. This result may be rationalized in terms of the differences in the bulk of the two molecules, due to which intercalation of TB may be restricted compared to TH. Thus, quenching results suggest comparative strength of intercalation based on the bulk of the molecules.

Viscosity measurements

The mode of binding of the dyes to helical ss poly(A) structure was investigated from viscosity measurements. Hydrodynamic measurements are sensitive to length changes and are regarded as one of the most critical test for elucidating the binding mode of small ligands to nucleic acids in solution.[35] The relative specific viscosity of the poly(A)-dye complexes increased as the dye/ poly(A) ratio increased and leveled of at a [dye]/[polynucleotide] > 0.5. Nevertheless, we note that since ss poly(A) has only stacked helical structure (no base pairing) a true intercalation model[35] where planar ligand molecules are fully sandwiched between hydrogen-bonded base pairs of double stranded DNA cannot be visualized. This data together with the quenching data and hypochromism in the absorbance spectrum supports an intercalation type of insertion of the dyes into the helical ss poly(A) structures.

Spectroscopic study by circular dichroism

Circular dichroism was used to understand and compare the conformational aspects of the interaction of the two dyes to ss poly(A) structure. The CD spectral changes of ss poly(A) on interaction with TH and TB in region 210-400 nm are depicted in Fig. 4a and 4b. Poly(A) has

REVISED MANUSCRIPT RA-ART-01-2014-000790

characteristic CD spectrum with sharp positive bands at 265 nm and 220 nm and a negative band at 248 nm (Spectrum 1 of Fig. 4 a,b). In the presence of the dyes ellipticities of both the positive peaks of poly(A) were remarkably perturbed resulting in a rapid decrease of the ellipticity, while the change in the negative band was not very strong. This indicates that the self-structured poly(A) has similar CD spectral characteristics although the bound dye had some influence on the absolute ellipticity values. A new negative band around 290 nm implies the alteration of poly(A) structure upon addition of the dyes, very similar to that reported for coralyne-poly(A) complexes by Xing et al.[2] It may be noted that the decrease of the long wavelength band ellipticity has been correlated to both helix winding angle and base pair twist.[36] More often, structural change from A-form to B-form and from B-form to C-form in double stranded DNA results in such large decrease of the long wavelength band ellipticity.[37] Although a direct correlation of the change in the magnitude of the bands with parameters of the helix are complicated, and beyond the scope of this paper, it can be assumed that an ordered structural transition like the formation of self structure is occurring and this may be promoted by the effective screening of the phosphate charges by the intercalatively bound positively charged dyes. This fact was further supported from salt dependent CD studies. Overall, the magnitude of the CD changes was more pronounced for TH compared to TB.

To examine the conformational aspects in more detail, the induced CD of the dyes complexed with poly(A) was studied in the region 300–700 nm where neither ss poly(A) nor the dyes have any CD spectra. The association of both the dyes, devoid of any optical activity, with poly(A) generated induced CD for the bound dye molecules. The study was conducted by keeping fixed concentration of the dyes and varying the concentration of poly(A) and the outcome is presented in Fig. 4 c,d. A single negative induced CD band (at 566 nm) was observed apart from the 310

REVISED MANUSCRIPT RA-ART-01-2014-000790

nm positive peak in both the cases. The ellipticity of these bands increased as the binding progressed. The presence of an induced CD band in the visible absorption region on complexation with poly(A) further established the strong environment of the bound molecules inside the poly(A) helix. Considering the similar shape of the induced CD observed in both cases, the intercalated aromatic ring of the dyes were most likely oriented parallel to the poly(A) axis with its long direction perpendicular to the base-pairs long axis.[38] Based on the intensity of the CD bands, the intercalation of TH with poly(A) appears to be stronger than with TB and this inference is in confirmation with the results from other spectroscopic experiments.

Self-structure formation in poly(A)

Self-assembled structure or self-structure formation is an important recently revealed aspect of many small molecule-poly(A) interactions.[1,2,11-13,17] Circular dichroism and optical melting experiments of poly(A) in the presence of the two dyes were performed to ascertain the capability of the dyes to induce self-structure in ss poly(A). Both the dyes induce a stable secondary structure with a cooperative melting temperature of ~60^{o}C, even though this RNA homopolymer is single-stranded in the absence of ligand. We also found cooperative melting of poly(A)-TH and poly(A)-TB complexes from optical melting (Fig. 5 a,b) and CD (Fig. 5 c,d) studies at 257 nm indicating the formation of self assembled structure. Self-assembled structure induction in poly(A) by planar molecules has been supported by intercalative geometry and the melting results confirm such helical organization induced by the dyes.

Salt dependent CD and absorbance studies: role of electrostatic interactions

Interaction between ss poly(A) and charged ligands like TH and TB may be sensitive to cation concentration as polyelectrolytic or electrostatic forces are predominant for the initial attraction of the ligand molecules to the poly(A). To ascertain the role of electrostatic interaction in the

REVISED MANUSCRIPT RA-ART-01-2014-000790

binding process, salt dependent binding studies were performed by CD and absorbance experiments at two other [Na^+] viz. 100 and 200 mM in addition to that done at 50 mM. We have observed that the conformational changes in poly(A) were more pronounced as the salt concentration enhanced. This was also followed by the higher intensity for the induced CD bands of the dyes in the complex. With increase in Na^+ concentration, self-assembled structure was favoured in poly(A) in the presence of these dyes. At 50, 100 and 200 mM of [Na+], the self structure was induced by at D/P of 0.6, 0.4 and 0.3, respectively, for TH and TB. Thus, shielding of the electrostatic charges in poly(A) appears to favor the self-assembled structure formation and hence the binding affinity increases due to favorable intercalation on to the self structured poly(A). The results are presented in Fig. 6 as CD studies revealing more conformational changes as the salt increased in the case of TH-poly(A) interaction. Similar observation was also obtained in the case of TB-poly(A) interaction (Fig. not shown).

To complement the CD studies, absorbance titration was performed at the above mentioned salt concentrations. From Fig. S3 the enhancement in the interaction phenomenon is obvious. The binding affinity values become more pronounced. The affinity values enhanced from (5.32±0.02) $\times 10^6\ M^{-1}$ to (9.02±0.03) $\times 10^6\ M^{-1}$ in case of TH and from (4.02±0.03) $\times 10^6\ M^{-1}$ to (8.33±0.02) $\times 10^6\ M^{-1}$ in the case of TB as the [Na^+] enhanced form 50 to 200 mM (table S2). An increase in the binding affinity of berberine and methylene blue with increase of salt concentration was previously reported.[7,17], but this study demonstrated for the first time that enhanced salt concentration leads to higher binding that leads to of self-structure formation at lower dye ratios.

Thermodynamic characterization of the dye-ss poly(A) interaction

Nucleic acid-targeted drug design requires accurate and rapid methods to directly obtain the thermodynamic information. This is facilitated from calorimetric studies that can provide

REVISED MANUSCRIPT RA-ART-01-2014-000790

information about the different thermodynamic parameters like standard molar Gibbs energy change (ΔG^o), standard molar enthalpy change (ΔH^o) and standard molar entropy change (ΔS^o) along with the stoichiometry and binding affinity. A direct titration protocol was followed where 150 µM of TH and 200 µM of TB sample were titrated into 20 µM of ss poly(A) solution at 20^{o}C. Fig. 7 a,b (upper panels) shows the representative raw ITC profiles at 20^{o}C. A single set of the identical sites model was used to fit the data that yielded the thermodynamic parameters for the binding. In the Fig. 7 c,d (lower panels), the resulting corrected injection heats are plotted against the respective molar ratios. The data points here represent the experimental injection heats and the solid lines denote the calculated fits of the data to the model. The corrected isotherms obtained at 20^{o}C for the binding of the dyes under investigation to the ss poly(A) sample was monophasic and revealed the binding to be exothermic. The binding affinity values obtained from ITC were in the order of 10^6 M^{-1}, which followed the same trend as those obtained from spectroscopic studies (Table 1); once again proving the fact that TH has a higher affinity towards ss poly(A) than TB. Similar to that of dye-DNA interaction[39], the exothermic heat effects can be explained by considering the interaction forces between the ss poly(A) and the dye molecule comprising hydrophobic, hydrogen bonds and electrostatic interactions. The direct attraction caused by these interactions between the dye molecule and poly(A) lead to exothermic effect which in turn reflected complex stability. The binding affinity and the other thermodynamic parameters of the complexation are given in Table 2.

Comparison with earlier reports of self structure formation

According to the report of Giri et al. planar conjugated DNA intercalating structures induced self-structure in poly(A) while buckled molecules like berberine, palmatine that are partial intercalators are ineffective in doing so.[11] Nevertheless, subsequent studies have proved that

REVISED MANUSCRIPT RA-ART-01-2014-000790

partial DNA intercalators like berberine and its many analogues also induced self structure.[15-16] Groove binders did not show any consistency in inducing this structural reorganization.[11] Another important criteria proposed from earlier reports is that cooperativity in the binding has a direct correlation to self-structure formation in poly(A).[11,17] In contrast, DNA intercalating sugar containing molecules daunomycin and aristololactam-β-D-glucoside could not induce self structure formation in poly(A) due to hindrance provided by the sugar moiety.[14] Previous reports showed that increase in salt concentration favoured higher binding of many small molecules to poly(A).[7,16,17] But so far there are no reports showing higher salt favoring better self-structure formation. The present study for the first time showed that with increase in salt concentration there is an ease of formation of self-assembled structure in poly(A). The negative enthalpy and positive entropy obtained here are very close to that obtained for planar molecules like proflavine and quinacrine which induced self structure in poly(A).[11] The present data correlate well with our previous data that self structure is favoured by planar intercalators and cooperative binding'[2,11-13,17] Furthermore the present data also advance that higher salt favoures self structure formation and leads to higher binding affinities. The exact reason of self-structure formation by small molecules although unclear the present study further advances our insights into this unique phenomenon.

Conclusions

The results presented here have confirmed that the phenothiazinium dyes TH and TB induce self-structure in ss poly(A) at neutral pH. Both the dyes have binding affinity to poly(A) of the order of 10^6 M^{-1}. The binding resulted in significant perturbation of the conformation of ss poly(A) leading to induction of optical activity in otherwise optically inactive dyes. The binding was stronger at higher salt concentrations in the range 50-200 mM [Na^+]. Concomitant with the

REVISED MANUSCRIPT RA-ART-01-2014-000790

affinity increase the ease of formation of self-assembled structure also enhanced. The binding was favored by both negative enthalpy and positive entropy changes, but to different extents. These findings present new insights in our understanding on the self-structure formation phenomena in poly(A) molecules.

Experimental section

Materials

Polyriboadenylic acid [poly(A)] as potassium salt was purchased from Sigma-Aldrich Corporation (St. Louis, MO, USA). The sampe was dialyzed into the experimental buffer. Concentration of poly(A) in terms of nucleotide phosphate (hereafter nucleotide) was determined by UV absorbance measurements at 257 nm using a molar extinction coefficient (ε) value of 10,000M^{-1} cm^{-1}.[40] Thionine (CAS No. 78338-22-4, Color Index Number: 52000, purity ~ 85%) and toluidine blue O (CAS No. 92-31-9, Color Index Number: 52040, purity ~ 80%) were products of Sigma-Aldrich and were recrystallized. TH was purified by recrystallizions from water followed by chromatography on alumina using chloroform as eluting agent. The sample showed no impurities upon subsequent repetition of the chromatographic steps.[41] The TB was purified by column chromatography on neutral alumina using ethanol:benzene (7:3 v/v) containing 0.4% glacial acetic acid. The fractions were pooled, concentrated under vacuum and crystallized. The crystals were dried in a vacuum desiccator at room temperature to give spectrally pure dye.[42] The concentrations were determined by absorbance measurement using molar extinction coefficients (ε) as follows: TH- 54,200 M^{-1} cm^{-1} at 598 nm and TB- 29,200 M^{-1} cm^{-1} at 618 nm. All other materials and chemicals used were of analytical grade. All experiments were conducted at 20°C in 50 mM sodium cacodylate buffer, pH 7.2. Deionized and doubled distilled water was used for buffer preparation.

REVISED MANUSCRIPT RA-ART-01-2014-000790

Preparation of the dye solutions

TH and TB (dyes hereafter in general) solutions were freshly prepared each day in the experimental buffer and kept protected in the dark to prevent any light induced photochemical changes. The overall concentration of the dyes in each experiment was kept at the lowest possible to prevent aggregate formation and adsorption to the cuvette walls. No deviation from Beer's law was observed in the concentration range used in this study.

Absorption and fluorescence spectral studies and evaluation of binding parameters

Absorption spectral studies were done on a Jasco V 660 double beam double monochromator spectrophotometer (Jasco International Co. Ltd., Hachioji, Japan) equipped with a thermoelectrically controlled cuvette holder and temperature controller in matched quartz cuvettes of 1 cm path length (Hellma, Germany) using the methodologies described in details earlier.[10,11] Steady state fluorescence measurements were performed on a Shimadzu RF-5301PC spectrofluorimeter (Shimadzu Corporation, Kyoto, Japan) in fluorescence free quartz cuvettes of 1 cm path length as described previously.[43] To avoid inner filter effects, it is generally advisable for the sample absorbance measured at the excitation wavelength not to exceed beyond 0.05 absorbance. In view of this fact, the concentration of TH and TB were kept at 0.8 μM (absorbance 0.043) and 1.6 μM (absorbance is 0.046), respectively, and fluorescence experiments were done. Thus, inner filter effect has been circumvented in this study. The excitation wavelength for TH and TB were 596 nm and 620 nm, respectively, and the emission intensity was monitored in the range 600-700 nm keeping an excitation and emission band pass of 5 nm at 20±1.0°C and after allowing a 5 min. equilibration time after each addition of aliquots of ss poly(A) solution into the dye solution.

REVISED MANUSCRIPT RA-ART-01-2014-000790

The Scatchard isotherms with positive slope at low r values were analyzed using the following McGhee-von Hippel equation for cooperative binding.[34]

$$\frac{r}{C_f} = K_i(1-nr)\times\left(\frac{(2\omega+1)(1-nr)+(r-R)}{2(\omega-1)(1-nr)}\right)^{(n-1)}\left(\frac{1-(n+1)r+R}{2(1-nr)}\right)^{2} \quad (1)$$

where, $R = \{[1-(n+1)r]^2 + 4\omega r(1-nr)\}^{\frac{1}{2}}$

where K_i is the intrinsic binding constant to an isolated binding site, 'n' is the number of base pairs excluded by the binding of a single dye molecule and ω is the cooperativity factor. All the binding data were analyzed using Origin 7.0 software (Microcal Inc., Northampton, MA, USA) to determine the best-fit parameters of K_i and 'n' to equation (1).

Determination of the binding stoichiometry

Job plot[44-46] methodology was employed to determine the binding stoichiometry from fluorescence spectroscopy described previously.[10-11] The fluorescence signal was recorded for mixture of solutions where the concentrations of both ss poly(A) and the dyes were varied keeping the sum of their concentration constant. The difference in fluorescence intensity (ΔF) of the dyes in the absence and presence of the ss poly(A) was plotted as a function of the input mole fraction of the dyes. The stoichiometry in terms of ss poly(A)-dye [$(1-\chi_{dye})/\chi_{dye}$] was obtained from the break points where χ_{dye} denotes the mole fraction of the respective dye. The results presented are average of three experiments.

Fluorescence quenching studies

Quenching studies were carried out with the anionic quenchers $[Fe(CN)_6]^{4-}$ as described previously.[47-48] The data were plotted as Stern-Volmer plots of relative fluorescence intensity (F_o/F) versus $[Fe(CN)_6]^{4-}$.

Viscosity measurements

REVISED MANUSCRIPT RA-ART-01-2014-000790

Viscosity measurements were made using a Cannon-Manning semi micro dilution viscometer type 75 (Cannon Instruments Co., State College, PA, USA) which was thermostated at 20±1°C.in a constant temperature bath. The ss poly(A) concentration was fixed at 700 μM while the dye concentration was varied and flow times with an accuracy of ±0.01 s were measured with an electronic stop watch; the mean values of three replicated measurements were used to evaluate viscosity (η) of the samples.[43,48-49]

$$\eta/\eta_o = \{(t_{complex} - t_o)/t_o\}/\{(t_{control} - t_o)/t_o\} \quad (2)$$

The values of relative specific viscosity $(\eta/\eta_o)^{1/3}$ were estimated where η_o and η are the specific viscosity contributions of poly(A) in the absence and in the presence of the dyes and $t_{complex}$, $t_{control}$ and t_o are the average flow times for the dye- poly(A) complexes, free poly(A) and buffer, respectively.

Spectropolarimetric studies

Circular dichroism (CD) spectra were acquired on a Jasco J815 unit (Jasco International Co. Ltd., Japan) equipped with a Jasco temperature controller (PFD 425L/15) as reported.[11] The molar ellipticity values [θ] are expressed in terms of either per nucleotide phosphate (210-400 nm) or per bound dye (300-500 nm).

CD melting profiles were obtained by heating the sample at a scan rate of 0.8°C/min and monitoring the CD signal at 257 nm. For the melting profiles, the ellipticity values are expressed in units of milli degrees.

Optical thermal melting studies

Absorbance versus temperature profiles (optical melting curves) of the complexes were measured on a Shimadzu Pharmaspec 1700 unit equipped with a Peltier controlled TMSPC-8 model microcell accessory (Shimadzu Corporation, Kyoto, Japan), as reported previously.[11,42]

REVISED MANUSCRIPT RA-ART-01-2014-000790

Isothermal titration calorimetry

A MicroCal VP-ITC unit (MicroCal, Inc., Northampton, MA, USA) was used for all ITC experiments. Protocols developed in our laboratory and described in details previously[10-11] were used for the dye- poly(A) titrations. A direct titration protocol of injecting aliquots of degassed dye solution from the rotating syringe (290 rpm) into the isothermal chamber containing the poly(A) solution (1.4235 mL) was employed. Corresponding control experiments to determine the heat of dilution of the dyes were also performed. The area under each heat burst curve was determined by integration using the Origin 7.0 software to give the measure of the heat associated with the injections. The control heat was subtracted from the heat of ss poly(A)-dye reaction to give the heat of dye-ss poly(A) binding. The heat of dilution of injecting the buffer into the poly(A) solution alone was found to be negligible. The resulting corrected injection heats were plotted as a function of molar ratio and fit with a model for one set of binding sites to provide the binding affinity (K_a), the binding stoichiometry (N) and the standard enthalpy of binding (ΔH^o). The standard molar Gibbs energy change (ΔG^o) and the entropic contribution to the binding ($T\Delta S^o$) were subsequently calculated from standard relationships.[50-51] The ITC unit was periodically calibrated and verified with water-water dilution experiments as per criteria of the manufacturer.

Acknowledgement

This work was supported by the Council of Scientific and Industrial Research (CSIR), Government of India network projects GenCODE (BSC0123). P. Paul is a NET-Senior Research Fellow of the CSIR. Authors thank all the colleagues of the Biophysical Chemistry Laboratory for their help and cooperation. We would like to thank the reviewers for their insightful comments on the paper, as these comments led us to an improvement of the work.

REVISED MANUSCRIPT RA-ART-01-2014-000790

Electronic supplementary information

†Electronic supplementary information (ESI) available. See DOI:XXX

REVISED MANUSCRIPT RA-ART-01-2014-000790

References

1 H. Xi, D. Gray, S. Kumar and D.P. Arya, *FEBS Lett.*, 2009, **583**, 2269-2275.

2 F. Xing, G. Song, J. Ren, J.B. Chaires and X. Qu, *FEBS Lett*., 2005, **579**, 5035-5039.

3 P. Centikol and N.V. Hud, *Nucleic Acids Res*., 2009, **37**, 611-621.

4 S.L. Topalian, S. Kaneko, M.I. Gonzales, G. Bond, Y. Ward and J. Manley, *Mol. Cell. Biol.*, 2001, **21**, 5614-5623.

5 W. Saenger, Principles of Nucleic Acid Structure, Springer-Verlag, New York, 1984.

6 A.G. Petrovic and P.L. Polavarapu, *J. Phys. Chem. B*, 2005, **109**, 23698-23705.

7 R.C. Yadav, G.Suresh Kumar, K. Bhadra, P. Giri, R. Sinha, S. Pal and M. Maiti, *Bioorg. Med. Chem.*, 2005, **13**, 165-174.

8 P. Giri, M. Hossain and G.Suresh Kumar, *Int. J. Biol. Macromol*., 2006, **39**, 210-221.

9 P. Giri, M. Hossain and G.Suresh Kumar, *Bioorg. Med. Chem. Lett.*, 2006, **16**, 2364-2368.

10 P. Giri and G.Suresh Kumar, *Biochim. Biophys. Acta*, 2007, **1770**, 1419-1426.

11 P. Giri and G.Suresh Kumar, *Arch. Biochem. Biophys*., 2008, **474**, 183-192.

12 P. Giri and G.Suresh Kumar, *Curr. Med. Chem.*, 2009, **16**, 965-987.

13 P. Giri and G.Suresh Kumar, *Mol. Biosyst.*, 2010, **6**, 81-88.

14 A. Das, K. Bhadra, B. Achari, P. Chakraborty and G.Suresh Kumar, *Biophys. Chem.*, 2011, **155**, 10-19.

15 M. M. Islam, A. Basu and G.Suresh Kumar, *Med. Chem. Commun*., 2011, **2**, 631-637.

16 A. Basu, P. Jaisankara and G.Suresh Kumar, *RSC Advances*, 2012, **2**, 7714-7723.

17 M. Hossain, A. Kabir and G.Suresh Kumar, *Dyes Pigments* 2012, **92**, 1376-1383.

REVISED MANUSCRIPT RA-ART-01-2014-000790

18 X. Long, S. Bi, X. Tao, Y. Wang and H. Zhao, *Spectrochim. Acta Part A*, 2004, **60**, 455-462.

19 E. Tuite and J.M. Kelly, *Biopolymers*, 1995, **35**, 419-433.

20 E.M. Tuite and J.M. Kelly, *J. Photochem. Photobiol. B*, 1993, **B21**, 103-124.

21 R. Briggs, *J. Gen. Physiol.*, 1951, 761-780.

22 J.C. Hunter, D. Burk and M.W. Woods, *J. Natl. Cancer Inst.*, 1967, **39**, 587-593.

23 Vugman and M.L.M. do Prado, *Arch. Pharmacol*., 1973, **279**, 173-184.

24 K. Zhao, H. Song, S. Zhuang, L. Dai, P. He and Y. Fang, *Electrochem. Comm.*, 2007, **9**, 65-70.

25 M. Keyvanfard, *Asian J. Chem.*, 2007, **19**, 4977-4984.

26 P. Hashemi, M. Hosseini, K. Zargoosh and K. Alizadeh, *Sens. Actuators B: Chemical*, 2011, **153**, 24-28.

27 A.J. Dunipace, R. Beaven, T. Noblitt, Y. Li, S. Zunt and G. Stookey, *Mutat. Res*., 1992, **279**, 255-259.

28 L.M. Popa and L. Bosch, *FEBS Lett.*, 1969, **4**, 143-146.

29 N. Kashef, G.R.S. Abadi and G.E. Djavid, *Photodiagn. Photodyn.*, 2012, **9**, 355-358.

30 A. Mashberg and H. Ephros, *Oral Surgery Oral Medicine Oral Pathology*, 1999, **87**, 527-528.

31 G. P. Wysocki, *Oral Surg. Oral Med. O.*, 1999, **87**, 527-528.

32 P. Paul and G.Suresh Kumar, *Spectrochim. Acta A.*, 2013, **107**, 303-310.

33 P. Paul and G.Suresh Kumar, *J. Haz. Mat.*, 2013, **263**, 735-745.

34 J.D. McGhee and P.H. Von Hippel, *J. Mol. Biol*., 1974, **86**, 469-489.

35 L.S. Lerman, *Proc. Natl. Acad. Sci. USA*, 1963, **49**, 94-102.

REVISED MANUSCRIPT RA-ART-01-2014-000790

36 M. R. Duff Jr, V.K. Mudhivarthi and C.V. Kumar, *J. Phys. Chem. B*, 2009, **113**, 1710-1721.

37 B. B. Johnson, K.S. Dahl, I. Tinoco Jr., V.I. Ivanov and V.B. Zhurkin, *Biochemistry.*, 1981, **20**, 73-78.

38 R. Lyng, T. Hard and B. Norden, *Biopolymers*, 1987, **26**, 1327-1345.

39 M. Gharagozlou and D.M. Boghaei, *Spectrochim. Acta A*, 2008, **71**, 1617-1622.

40 C. Ciatto, M.L. D'Amico, G. Natile, F. Secco and M. Venturini, *Biophys. J.*, 1999, **77**, 2717-2724.

41 A. Shepp, S. Chaberek and R. MacNeil, *J. Phys. Chem.*, 1962, **66**, 2563-2569.

42 J. Jebaramya, M. Ilanchelian and S. Prabahar, *Digest J. Nanomater. Biostruct.*, 2009, **4**, 789-797.

43 R. Sinha, M.M. Islam, K. Bhadra, G.Suresh Kumar and A. Banerjee, *Bioorg. Med. Chem.*, 2006, **14**, 800-814.

44 P. Job, Ann. Chim. 9 (1928) 113-203.

45 C.Y. Huang, S.P. Colowick, Methods Enzymol. Academic Press, N.O. Kaplan (Eds.). 87 (1982) 509-525.

46 Z.D. Hill and M. Patrick, *J. Chem. Educ.*, 1986, **63**, 162-167.

47 M.M. Islam, S.R. Chowdhury and G.Suresh Kumar, *J. Phys. Chem. B*, 2009, **113**, 1210-1224.

48 R. Sinha and G.Suresh Kumar, *J. Phys. Chem. B*, 2009, **113**, 13410–13420.

49 S. Das and G.Suresh Kumar, *J. Mol. Struct.*, 2008, **872**, 56-63.

50 M.M. Islam, R. Sinha and G.Suresh Kumar, *Biophys. Chem.*, 2007, **125**, 508-520.

REVISED MANUSCRIPT RA-ART-01-2014-000790

524 51 M. M. Islam, P. Pandya, S.R. Chowdhury, S. Kumar and G.Suresh Kumar, *J. Mol. Struct.*, 2008, **891**, 498-507.

526

REVISED MANUSCRIPT RA-ART-01-2014-000790

FIGURE CAPTIONS

Fig. 1. Chemical structure of (a) thionine and (b) toluidine blue O.

Fig. 2. Representative absorption spectra of (a) TH (1.25 μM) treated with 0, 1.25, 2.5, 5.0, 8.75, 12.5, 16.25, 18.75, 21.25 μM (curves 1-9) of ss poly(A) and (b) TB (2.3 μM) treated with 0, 2.3, 4.6, 9.2, 16.1, 23.3, 29.9, 36.8, 43.7 μM (curves 1-9) of ss poly(A).

Representative steady state fluorescence emission spectrum of (c) TH (0.8 μM) treated with 0, 0.8, 1.6, 2.4, 4.0, 6.4, 9.6, 12.0, 14.4 μM (curves 1-9) of ss poly(A) and (d) TB (1.6 μM) treated with 0, 1.6, 3.2, 6.4, 12.8, 19.2, 24.0, 28.8, 32 μM (curves 1-9) of ss poly(A).

Fig. 3. Representative Scatchard plots of the binding of TH (■) and TB (●) to ss poly(A) obtained from spectrophotometric (a,b) and spectrofluorimetric (c,d) titrations.

Fig. 4. Representative intrinsic circular dichroism spectra of 60 μM ss poly(A) treated with (a) 0, 6, 12, 24, 36, 48, 60 μM of TH (curves 1-7) and (b) 0, 6, 12, 24, 36, 48, 60 μM of TB (curves 1-7). The expressed molar ellipticity (θ) values are based on ss poly(A) concentration.

Inset: Representative induced circular dichroism spectra of (c) 50 μM of TH treated with 50, 100, 200, 300, 400, 450, 500 μM and (d) 50 μM of TB treated with 50, 100, 200, 300, 400, 450, 500 μM of ss poly(A) as represented by curves (1-7). The expressed molar ellipticity (θ) values are based on the concentration of the dyes.

Fig. 5. Optical thermal melting profiles of poly(A) (○) and (a) TH-poly(A) complex (■) and (b) TB-poly(A) complex (●) monitored at 257 nm. Circular dichroism melting profiles of poly(A) (inset of Fig. 8d) and (c) TH-poly(A) complex and (d) TB-poly(A) complex monitored at wavelength 257 nm.

REVISED MANUSCRIPT RA-ART-01-2014-000790

Fig. 6. Representative circular dichroism spectra resulting from interaction of poly(A) (60 μM) treated with 0, 6, 12, 24, 36 μM (curves 1-5) of TH in (a) 50 mM [Na^+], (b) 100 mM [Na^+] and (c) 200 mM [Na^+] sodium cacodylate buffer, pH 7.2. Inset: Induced CD spectra of 50 μM of TH treated with 50, 100, 200, 300, 400 μM (curves 1-5) of ss poly(A) in (a) 50 mM [Na^+] (b) 100 mM [Na^+] and (c) 200 mM [Na^+] sodium cacodylate buffer.

Fig. 7. ITC profiles for the titration of (a) TH (■) and (b) TB (●) with ss poly(A) at 20^{o}C in 50 mM sodium-cacodylate buffer of pH 7.2. The top panels represent the raw data for the sequential injection of the dyes into ss poly(A) and the bottom panels show the integrated heat data after correction of heat of dilution against the molar ratio of ss poly(A) /dye. The data points (■,TH-ss poly(A) and ●, TB - ss poly(A) are the experimental injection heats and the solid lines represent the best-fit data.

REVISED MANUSCRIPT RA-ART-01-2014-000790

Table 1: Binding parameters for the complexation of the two dyes with ss poly(A) evaluated from Scatchard analysis of the absorbance and fluorescence titration data[a].

Dyes studied	Absorbance				Fluorescence			
	$K\times10^{-5}$ $(M^{-1})^b$	n	ω	$K_i\times10^{-6}$ $(M^{-1})^b$	$K\times10^{-5}$ $(M^{-1})^b$	n	ω	$K_i\times10^{-6}$ $(M^{-1})^b$
TH	2.66±0.02	2.23	20	5.32±0.02	2.28±0.04	2.43	23	5.24±0.04
TB	0.67±0.03	2.58	60	4.02±0.03	0.64±0.01	2.50	62	3.97±0.01

[a]Average of four determinations. [b]Binding constants (*K*) and the number of binding sites (n) refer to solution conditions of 50 mM cacodylate buffer, pH 7.2 at 20°C. ω is the cooperativity factor.

REVISED MANUSCRIPT RA-ART-01-2014-000790

Table 2: Temperature dependent isothermal titration calorimetric data for the binding of TH and TB to ss poly(A) at pH 7.2.

Dye	T (^{o}C)	$K_a \times 10^{-6}$ (M^{-1})	n (1/N)	ΔG^{o} (kcal/mole)	ΔH^{o} (kcal/mole)	$T\Delta S^{o}$ (kcal/mole)
TH	20	4.96±0.05	2.38	-8.81±0.05	-4.67±0.05	4.14±0.05
TB	20	3.58±0.02	2.56	-8.78±0.02	-3.13±0.02	5.65±0.02

The data in this table were derived from ITC experiments conducted in 50 mM cacodylate buffer, pH 7.2 and are average of four determinations. T denotes the temperatures studied. K_a, the binding affinity and ΔH^{o}, the enthalpy change were determined from ITC profiles fitting to Origin 7 software as described in the text. n is the site size. The values of ΔG^{o}, Gibbs energy change and $T\Delta S^{o}$, the entropy contribution were determined using the equations $\Delta G^{o} = -$ RT ln K_a, and $T\Delta S^{o} = \Delta H^{o} - \Delta G^{o}$. All the ITC profiles were fit to a model of single binding sites. Uncertainties correspond to regression standard errors.

REVISED MANUSCRIPT RA-ART-01-2014-000790

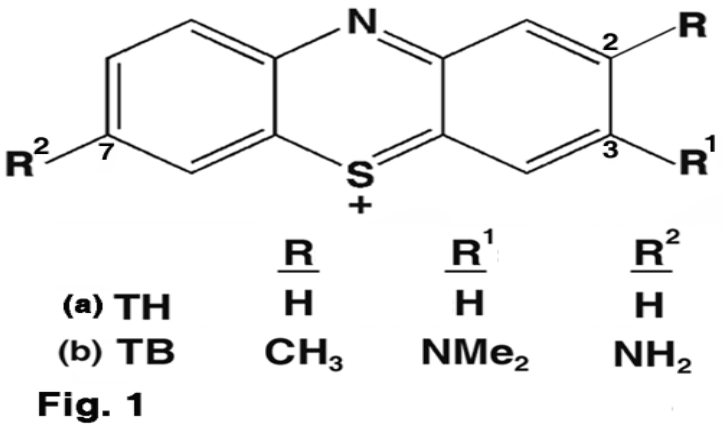

Fig. 1. Chemical structure of (a) thionine and (b) toluidine blue O.

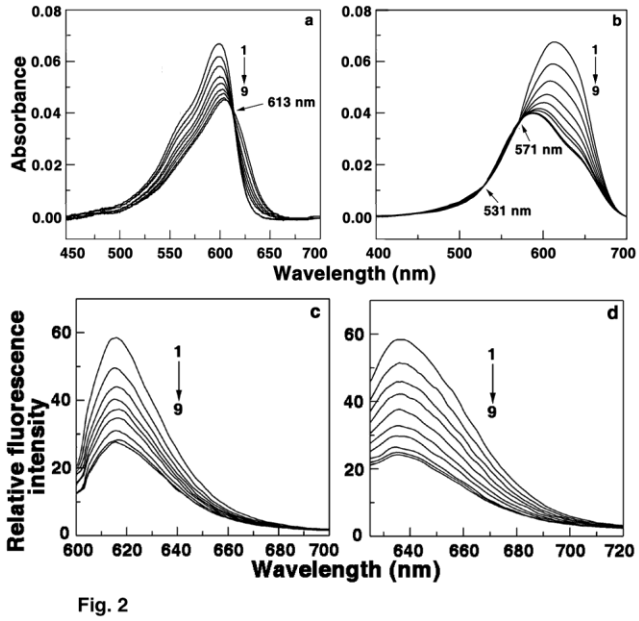

Fig. 2. Representative absorption spectra of (a) TH (1.25 μM) treated with 0, 1.25, 2.5, 5.0, 8.75, 12.5, 16.25, 18.75, 21.25 μM (curves 1-9) of ss poly(A) and (b) TB (2.3 μM) treated with 0, 2.3, 4.6, 9.2, 16.1, 23.3, 29.9, 36.8, 43.7 μM (curves 1-9) of ss poly(A).

REVISED MANUSCRIPT RA-ART-01-2014-000790

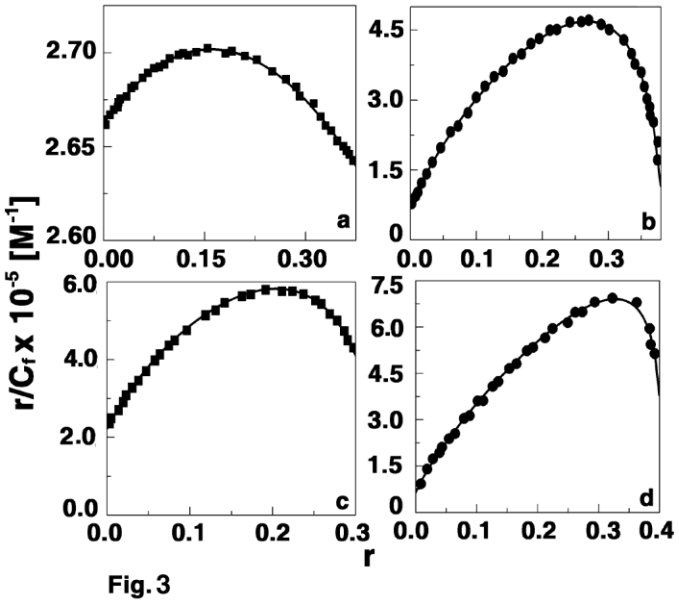

Fig. 3. Representative Scatchard plots of the binding of TH (■) and TB (●) to ss poly(A) obtained from spectrophotometric (a,b) and spectrofluorimetric (c,d) titrations.

REVISED MANUSCRIPT RA-ART-01-2014-000790

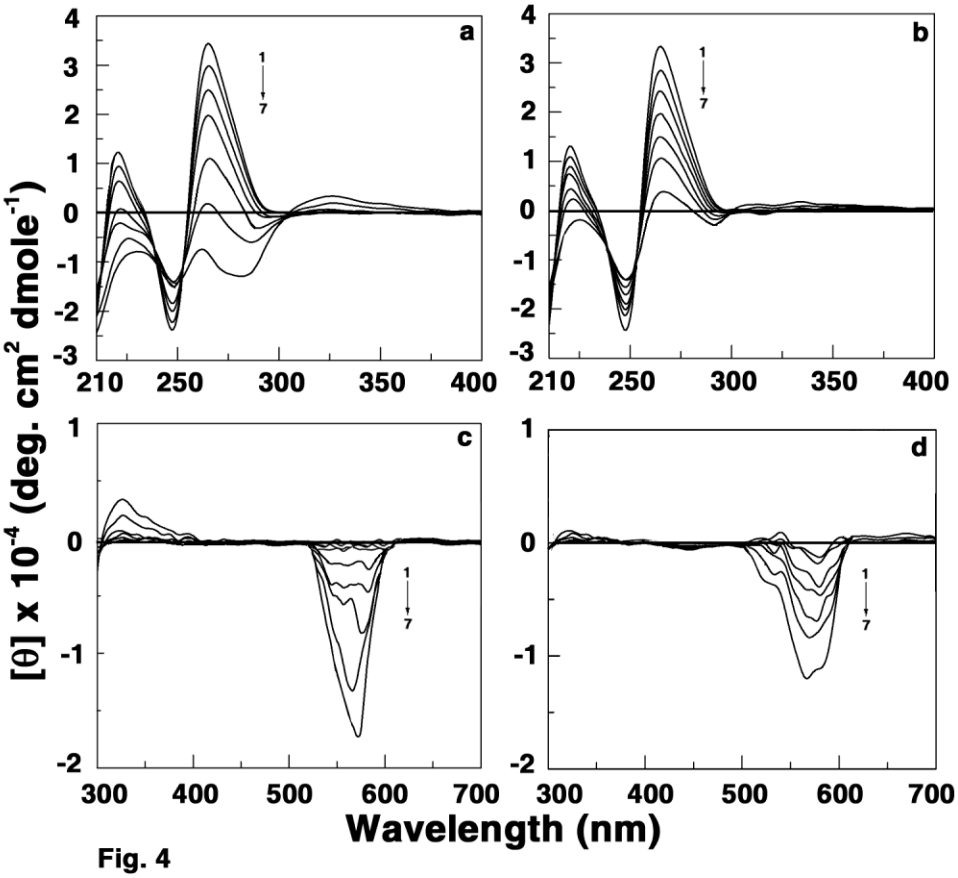

Fig. 4

Fig. 4. Representative intrinsic circular dichroism spectra of 60 μM ss poly(A) treated with (a) 0, 6, 12, 24, 36, 48, 60 μM of TH (curves 1-7) and (b) 0, 6, 12, 24, 36, 48, 60 μM of TB (curves 1-7). The expressed molar ellipticity (θ) values are based on ss poly(A) concentration.

Inset: Representative induced circular dichroism spectra of (c) 50 μM of TH treated with 50, 100, 200, 300, 400, 450, 500 μM and (d) 50 μM of TB treated with 50, 100, 200, 300, 400, 450, 500 μM of ss poly(A) as represented by curves (1-7). The expressed molar ellipticity (θ) values are based on the concentration of the dyes.

REVISED MANUSCRIPT RA-ART-01-2014-000790

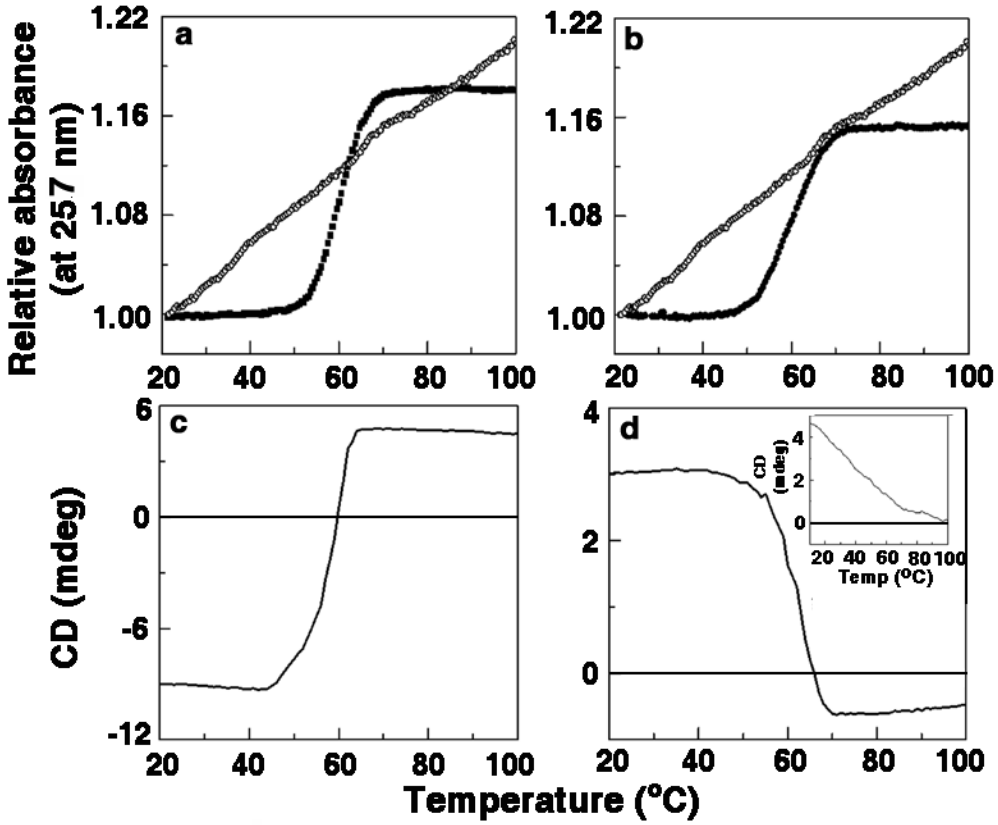

Fig. 5

Fig. 5. Optical thermal melting profiles of poly(A) (○) and (a) TH-poly(A) complex (■) and (b) TB-poly(A) complex (●) monitored at 257 nm. Circular dichroism melting profiles of poly(A) (inset of Fig. 8d) and (c) TH-poly(A) complex and (d) TB-poly(A) complex monitored at wavelength 257 nm.

REVISED MANUSCRIPT RA-ART-01-2014-000790

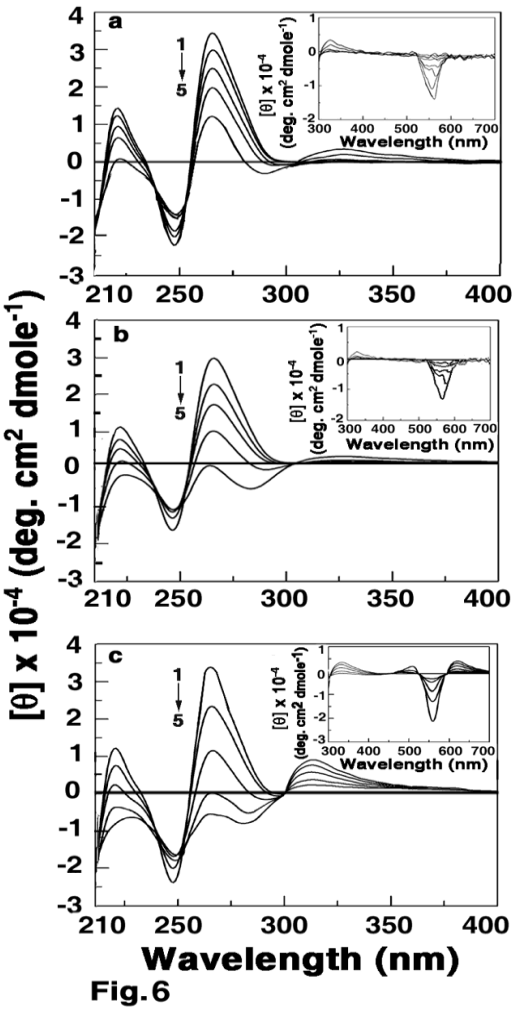

Fig. 6. Representative circular dichroism spectra resulting from interaction of poly(A) (60 μM) treated with 0, 6, 12, 24, 36 μM (curves 1-5) of TH in (a) 50 mM [Na^+], (b) 100 mM [Na^+] and (c) 200 mM [Na^+] sodium cacodylate buffer, pH 7.2. Inset: Induced CD spectra of 50 μM of TH treated with 50, 100, 200, 300, 400 μM (curves 1-5) of ss poly(A) in (a) 50 mM [Na^+] (b) 100 mM [Na^+] and (c) 200 mM [Na^+] sodium cacodylate buffer.

REVISED MANUSCRIPT RA-ART-01-2014-000790

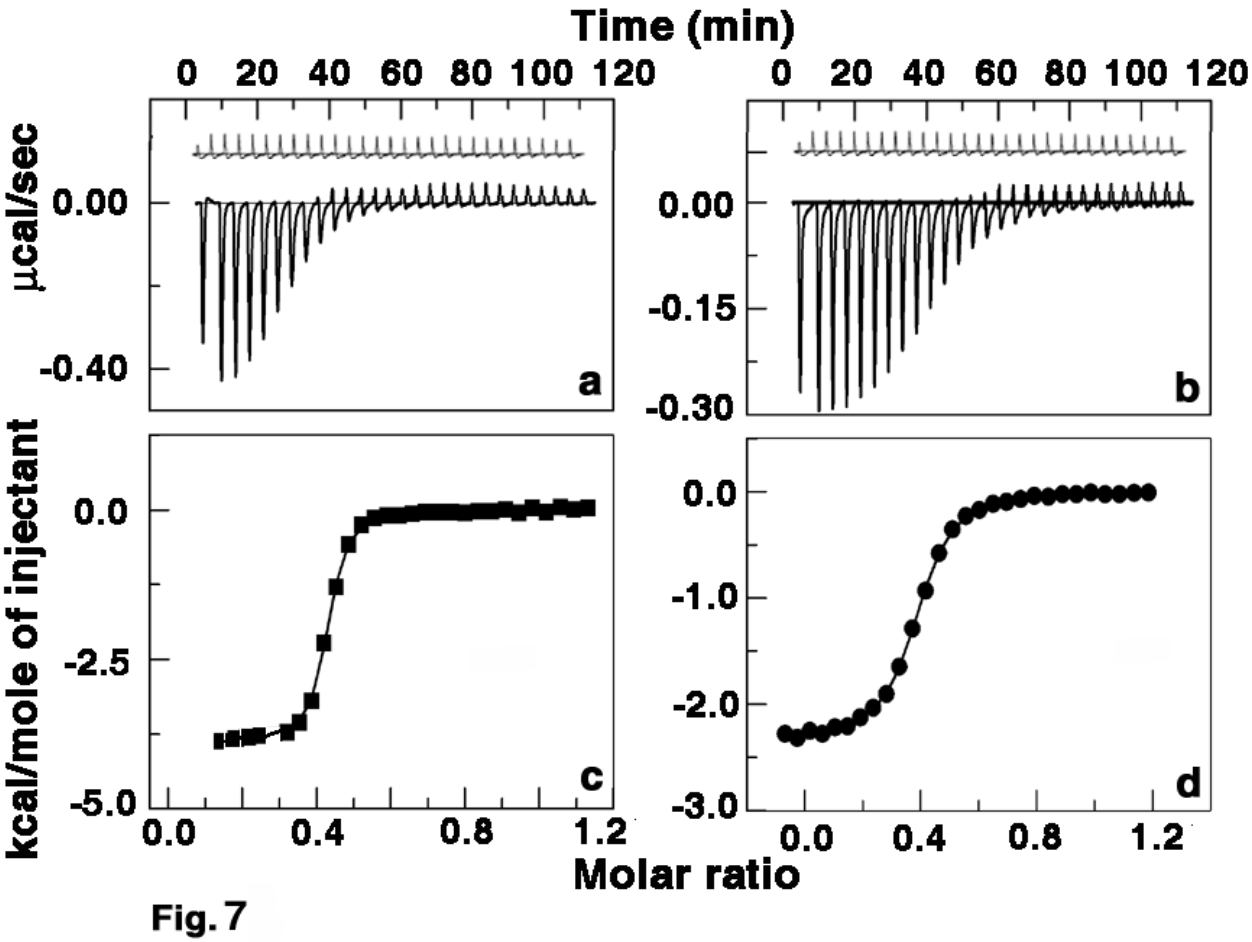

Fig. 7. ITC profiles for the titration of (a) TH (■) and (b) TB (●) with ss poly(A) at 20°C in 50 mM sodium-cacodylate buffer of pH 7.2. The top panels represent the raw data for the sequential injection of the dyes into ss poly(A) and the bottom panels show the integrated heat data after correction of heat of dilution against the molar ratio of ss poly(A) /dye. The data points (■,TH-ss poly(A) and ●, TB - ss poly(A) are the experimental injection heats and the solid lines represent the best-fit data.

REVISED MANUSCRIPT RA-ART-01-2014-000790

Supplementary Data

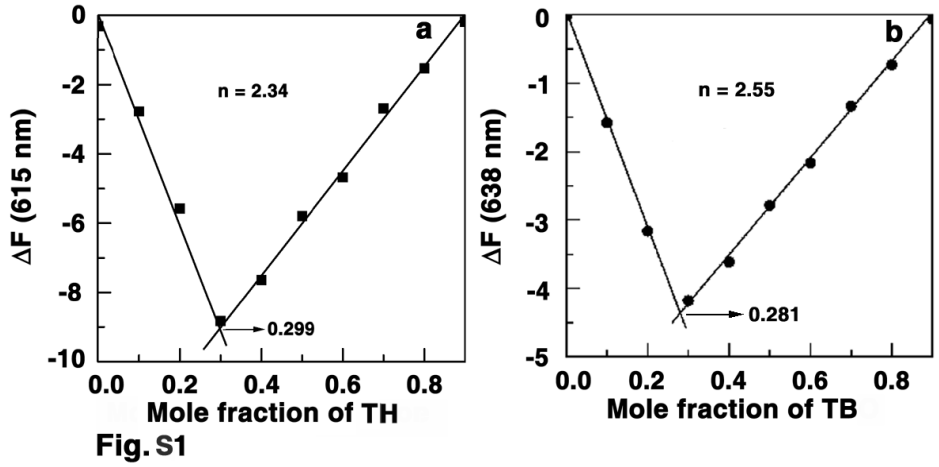

Fig. S1. Job plot for the binding of (a) TH (■) and (b) TB (●) to ss poly(A).

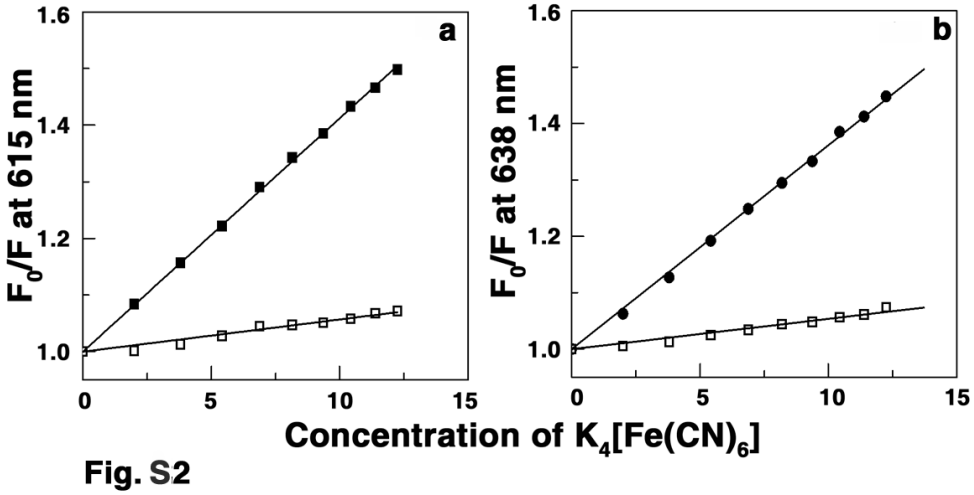

Fig. S2. Stern-Volmer plots for the quenching of (a) TH (■) and (b) TB (●) and complexes of TH- ss poly(A) (□) and TB- ss poly(A) (○) with increasing concentration of $K_4[Fe(CN)_6]$.

REVISED MANUSCRIPT RA-ART-01-2014-000790

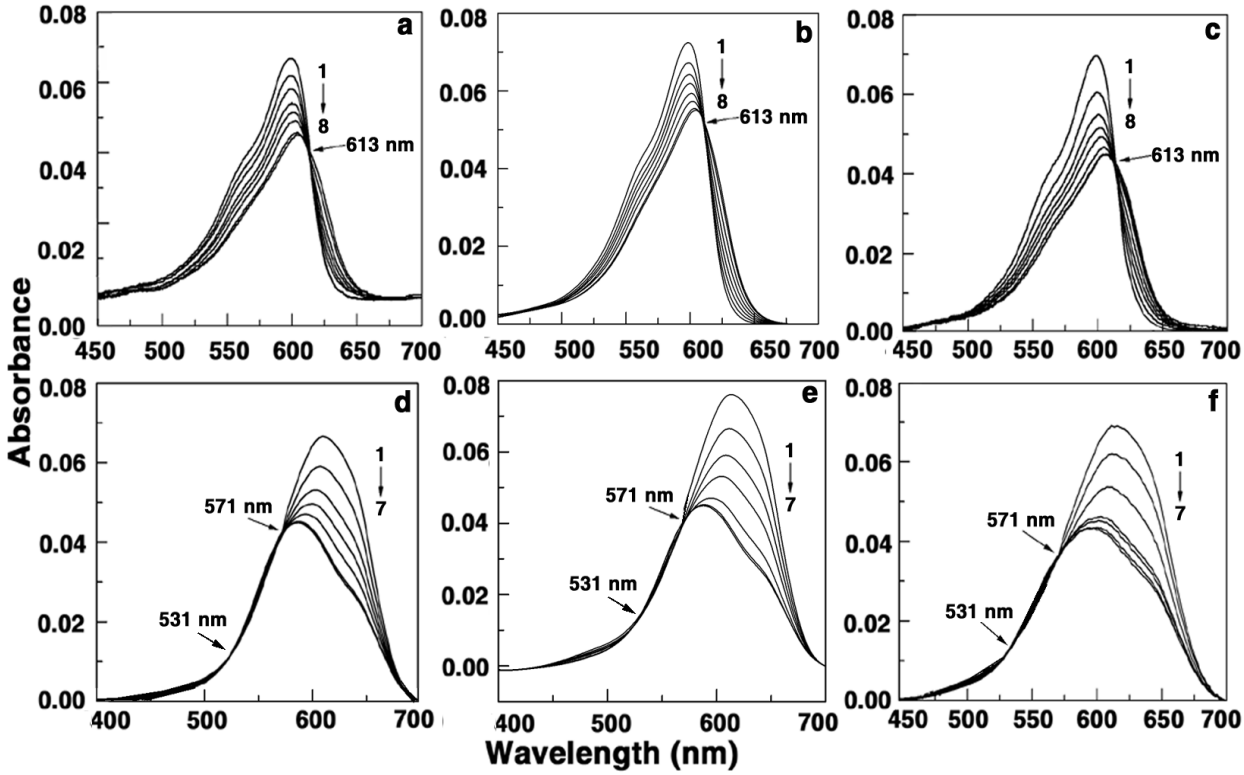

Fig. S3

Fig. S3. Absorbance titration of TH (upper panels) and TB (lower panels) in (a,d) 50 mM, (b,e) 100 mM and (c,f) 200 mM [Na^+] concentrations.

REVISED MANUSCRIPT RA-ART-01-2014-000790

Table S1: Summary of the optical properties of free and ss poly (A) bound dyes[a].

Parameter	TH	TB
	Absorbance	
λ_{max} (free)	598	618
λ_{max} (bound)	606	587
λ_{iso} [b]	613	531, 571
ε_f (at λ_{max})	54,200	29,200
ε_b (at λ_{max})	40,390 (598)	14,270 (618)
ε_{iso} (at λ_{iso})	39,428 (613)	14,123 (571)
	Fluorescence	
λ_{max} (excitation)	596	620
λ_{max} (emission)	615	638

[a]Units: λ (wavelength) nm; ε (molar extinction coefficient) M^{-1} cm^{-1}. [b]Wavelengths at the isosbestic points.

REVISED MANUSCRIPT RA-ART-01-2014-000790

Table S2: Binding parameters for the complexation of the two dyes with ss poly(A) evaluated from Scatchard analysis of the absorbance titration data[a].

Dyes studied	Salt	$K\times10^{-5}$ $(M^{-1})^b$	n	ω	$K\times10^{-6}$ $(M^{-1})^b$
TH	50	2.66±0.02	2.23	20	5.32±0.02
	100	3.21±0.04	2.21	25	8.02±0.04
	200	3.11±0.03	2.19	29	9.02±0.03
TB	50	0.67±0.03	2.58	60	4.02±0.03
	100	0.99±0.01	2.51	71	7.03±0.01
	200	1.11±0.02	2.44	75	8.33±0.02

[a]Average of four determinations. [b]Binding constants (*K*) and the number of binding sites (n) conducted in sodium cacodylate buffer of (50, 100 and 200) mM [Na^+], pH 7.2. ω is the cooperativity factor.

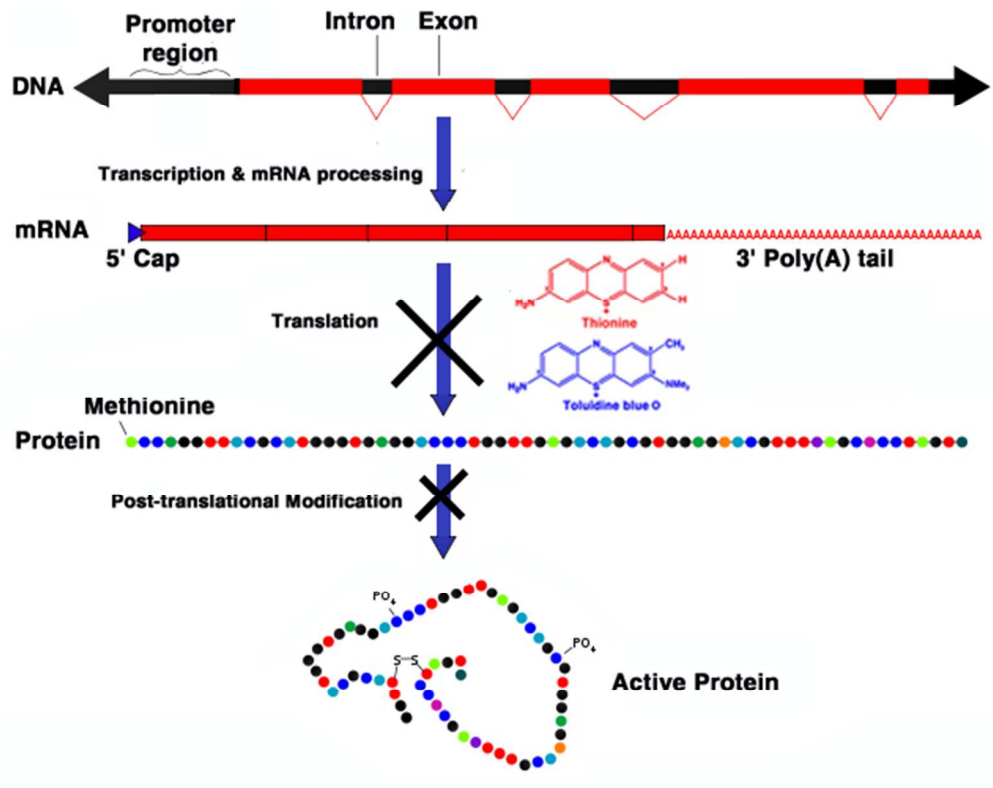

Thionine and Toluidine blue targeting poly(A)
224x175mm (72 x 72 DPI)